JOURNAL OF COLLOID AND INTERFACE SCIENCE **183,** 214–222 (1996)
ARTICLE NO. 0536

Solution to the Linearized Poisson–Boltzmann Equation for a Spheroidal Surface under a General Surface Condition

JYH-PING HSU[1] AND BO-TAU LIU

Department of Chemical Engineering, National Taiwan University, Taipei, Taiwan 10617, Republic of China

Received January 26, 1996; accepted May 29, 1996

The Poisson–Boltzmann equation describing the electrical potential distribution around a charged spheroidal surface in an electrolyte solution is solved analytically under the Debye–Huckel condition. A general boundary value problem is discussed in which an arbitrary combination of potential and charge density is specified at the surface. The method of reflections is proposed for the resolution of the governing Poisson–Boltzmann equation. The conventional constant potential (Dirichlet) problem and constant surface charge (Neumann) problem can be recovered as special cases of the present model. The problem of nonuniformly distributed potential/charges over a surface is also analyzed. A typical example in practice is that the distribution of charges is patchwise. We show that neglecting the nonuniformity of the charged condition over a surface may lead to a significant deviation. © 1996 Academic Press, Inc.

Key Words: **surface, charged, spheroidal, in electrolyte solution; Poisson–Boltzmann equation, linearized; surface condition, mixed potential and charge density, nonuniform; analytical solution, spheroidal wave functions, reflection method.**

1. INTRODUCTION

When a charged surface is immersed in an electrolyte solution an electrical potential gradient is established in the liquid phase. The distribution of electrical potential at equilibrium is described by the Poisson–Boltzmann equation (PBE) (1). In general, due to its nonlinearity, solving a PBE analytically is nontrivial. This difficulty, however, can be alleviated by assuming that the electrical potential of the system under consideration is low, i.e., the Debye–Huckel condition. In this case, a PBE can be approximated by a linear expression. The Debye–Huckel condition is satisfactory for a surface potential on the order of 25 mV, a level which is reasonable for most of the charged surfaces in practice.

Previous efforts for the resolution of a PBE were mainly limited to simple geometries such as infinite plates, long cylinders, and spheres. Although the mathematical treatment becomes much simpler, using these one-dimensional simulations can be unrealistic for a wide class of dispersed entities. Biocolloids, for instance, can be rod-like, olivary, and various other shapes. Attempts were made to extend the results for simple surfaces to spheroidal surfaces (2–4). The analyses, however, were limited to thin electrical double layers. This is largely due to the complicated nature of spheroidal coordinates and the spheroidal wave functions involved in the expression of electrical potential distribution. Although spheroidal wave functions have been investigated extensively in the literature (5, 6), their applications in the description of charged surfaces in electrolyte solutions are still very limited. Yoon and Kim (7) analyzed the electrophoretic phenomena of spheroidal particles by employing these functions. The eigenvalues and the coefficients associated with the solution to the two-dimensional electrical potential distribution needed to be evaluated through finding the roots of a transcendental equation. A more explicit and straightforward approach was suggested by Hsu and Liu (8) to the description of two-dimensional electrical potential distributions for spheroidal surfaces.

More often than not, a charged surface is assumed to be maintained at either constant potential or constant charge density. Furthermore, the distributions of potential and charges are uniform over the surface. Although these conditions may be appropriate to some special surfaces, the situation in practice can be far more complicated. For example, the basal face of a kaolin particle in a weak acidic solution is negatively charged, and its edge face is positively charged (9). The surfaces of many biocolloids bear various functional groups. The surface condition of such a particle depends largely on the degree of dissociation of these functional groups. In general, the degree of dissociation is a function of the electrical potential distribution around the particle (10–12). When a particle approaches a charged surface, the surface condition of the particle will vary with the position. In other words, the interaction between a particle and a charged surface may lead to a nonuniform surface charge distribution. Polymer-induced flocculation is another example which may lead to a nonuniform surface condition.

[1] To whom correspondence should be addressed.

0021-9797/96 $18.00

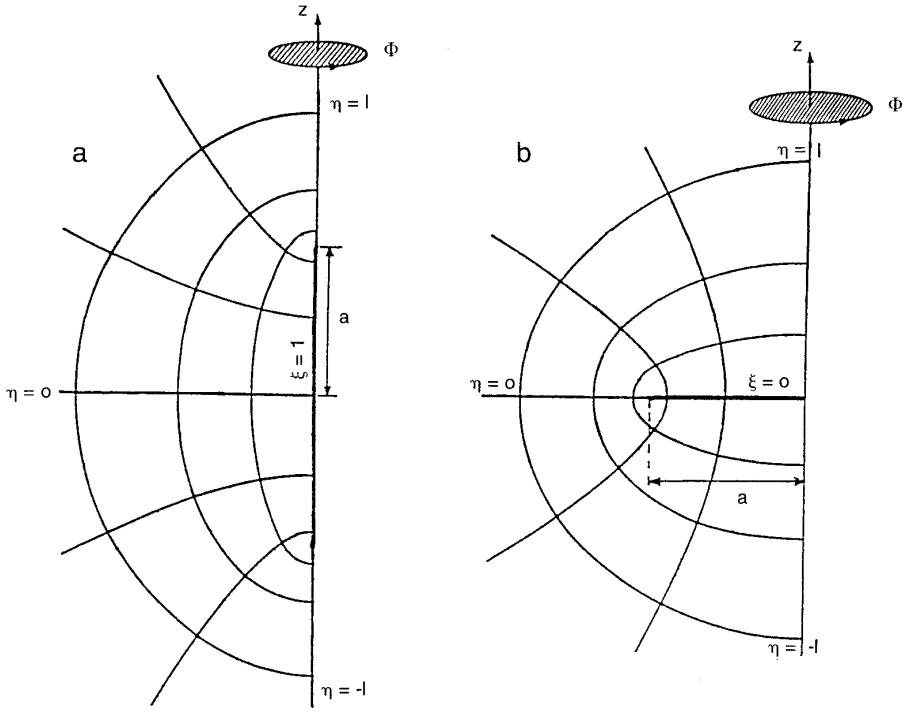

FIG. 1. Schematic representation of spheroidal coordinates: (a) prolate spheroid; (b) oblate spheroid.

In this case, the adsorption of cationic or anionic polymers to surfaces of dispersed colloidal particles leads to patchwise distribution of charges over the surfaces (13). Apparently, an extension of the conventional constant potential/charge density expression to a more realistic model, which is capable of taking various boundary conditions into account, is highly desirable.

In the present study, the linearized PBE for the case of a spheroidal surface is discussed. We consider a general boundary value problem in which an arbitrary combination of potential and charge density is specified at the surface.

2. MODELING

The electrical potential distribution around a charged surface in an electrolyte solution is described by the Poisson–Boltzmann equation. Under the Debye–Huckel condition, we have

$$\nabla^2 y = \kappa^2 y, \qquad [1]$$

where

$$y = e\psi/k_B T \qquad [1a]$$

$$\kappa^2 = 8\pi e^2 I/\epsilon k_B T. \qquad [1b]$$

In these expressions, ∇ denotes the Laplace operator, ψ is the electrical potential, ϵ is the dielectric constant, κ and k_B are the reciprocal Debye length and the Boltzmann constant, respectively, T is the absolute temperature, and e and I are, respectively, the elementary charge and the ionic strength. By referring to Fig. 1, we consider a general spheroidal particle with ξ, η, and Φ representing the radial, the angle, and the rotation coordinates, respectively. Here, a denotes the distance between the focus and the center of the particle. In this case Eq. [1] can be written as (14)

$$\frac{\partial}{\partial\eta}\left[(1-\eta^2)\frac{\partial y}{\partial\eta}\right] + \frac{\partial}{\partial\xi}\left[(\xi^2 - j)\frac{\partial y}{\partial\xi}\right] + \frac{\xi^2 - j\eta^2}{(\xi^2 - j)(1-\eta^2)}\frac{\partial^2 y}{\partial\Phi^2} - c^2(\xi^2 - j\eta^2)y = 0$$

$$(1+j)/2 \leqslant \xi < \infty, \quad -1 \leqslant \eta \leqslant 1, \quad 0 \leqslant \Phi \leqslant 2\pi, \qquad [2]$$

where $c = \kappa a$ and j is an index parameter ($j = 1$ for prolate spheroid, $j = -1$ for oblate spheroid). Note that since the expression for the oblate spheroid and that for the prolate spheroid can be obtained from each other by letting $\xi = \pm i\xi$, $c = \mp ic$, and $i = \sqrt{-1}$ in Eq. [2a], solving one of the two problems is enough. Assuming that

$$y = \Sigma R_{mn}(\xi) S_{mn}(\eta) \exp(im\Phi), \qquad [3]$$

Eq. [2] gives

$$\frac{d}{d\eta}\left[(1-\eta^2)\frac{dS_{mn}}{d\eta}\right] + \left(\lambda_{mn} + jc^2\eta^2 - \frac{m^2}{1-\eta^2}\right)S_{mn} = 0 \quad [3a]$$

$$\frac{d}{d\xi}\left[(1-j\xi^2)\frac{dR_{mn}}{d\xi}\right] + j\left(\lambda_{mn} + c^2\xi^2 - \frac{m^2}{1-j\xi^2}\right)R_{mn} = 0, \quad [3b]$$

where S_{mn} and R_{mn} are the eigenfunctions associated with eigenvalue λ_{mn}.

A. Angle Function S_{mn}

Equation [3b] suggests that if c^2 vanishes, the solutions to the resultant expression are the associated Legendre functions of the first kind of order m with degree n. This leads to the idea of expanding the solution of Eq. [3a] into a perturbation series in terms of c^2. It can be shown that (see Appendix A)

$$S_{mn}(\eta) = \sum_{s=0,1}^{\infty} A_{mn,s} P_{m+s}^{m}(\eta) \quad [4]$$

and

$$A_{mn,s} = \sum_{r=0}^{\infty} a_{mn,r,s}(jc^2), \quad [4a]$$

where s is even if $(n-m)$ is even, and is odd if $(n-m)$ is odd. Here, $\lambda_{mn,r}$ and $a_{mn,r,s}$ can be evaluated by the following recursive relations:

$$\lambda_{mn,r} = -[\alpha(n-m)a_{mn,r-1,n-m+2} + \beta(n-m)a_{mn,r-1,n-m} + \gamma(n-m)a_{mn,r-1,n-m-2}] \quad [5a]$$

$$a_{mn,r,s} = \frac{1}{(s+m)(s+m+1) - \lambda_{mn,0}}\{\alpha(s)a_{mn,r-1,s+2} + \beta(s)a_{mn,r-1,s} + \gamma(s)a_{mn,r-1,s-2} + \sum_{p=1}^{r-1}\lambda_{mn,p}a_{mn,r-p,s}\}, \quad s \neq n \quad [5b]$$

$$a_{mn,r,s} = 0, \quad s = n. \quad [5c]$$

In these expressions,

$$\alpha(s) = \frac{(s+2m+2)(s+2m+1)}{(2s+2m+5)(2s+2m+3)} \quad [5d]$$

$$\beta(s) = \frac{2s^2 + 4sm + 2s + 2m - 1}{(2s+2m-1)(2s+2m+3)} \quad [5e]$$

$$\gamma(s) = \frac{s(s-1)}{(2s+2m-3)(2s+2m-1)}. \quad [5f]$$

B. Radial Function R_{mn}

Although the equations governing the angle function, Eq. [3a], and that governing the radial function, Eq. [3b], are similar to each other, R_{mn} may not take a form similar to that of S_{mn}. This is because their domains are different: $(1+j)/2 \leqslant \xi < \infty$ for the former, and $-1 \leqslant \eta \leqslant 1$ for the latter. One possible approach to determine R_{mn} is to define the integral transform with a symmetric kernel (5),

$$R_n(\xi) = \frac{\pi}{2}\int_1^{\infty} (jc)^m \exp(-c\xi\eta) \times (j\xi^2 - 1)^{m/2}(1-\eta^2)^{m/2} S_{mn}(\eta)\, d\eta. \quad [6]$$

Based on the properties of the associated Legendre function and the relation (15, 16)

$$\int_1^{\infty} \exp(-xt)(t^2-1)^n dt = \frac{2^{n+1}n!}{\pi x^n} K_n(x), \quad [7]$$

it can be shown that

$$R_{mn}(c, \xi) = \sum_{s=0,1}^{\infty} A_{mn,r,s}\left(\frac{j\xi^2 - 1}{\xi^2}\right)^{m/2} \frac{(2m+s)!}{s!} K_n(c\xi). \quad [8]$$

Here, K_n is the modified spherical Bessel function of the third kind of order n (17), which can be expressed as

$$K_n(x) = \sqrt{\frac{\pi}{2x}}\, k_{n+1/2}(x), \quad [9]$$

where $k_{n+1/2}(x)$ is the modified Bessel function of the second kind. Note that if $c\xi$ is small, K_n approaches infinity and Eq. [8] diverges. In this case another expression for R_{mn} is necessary. According to Aoi (16), if V is a solution to Eq. [1], then the radial function can be expressed as

$$R_{mn}(\xi) = \int_{\Omega} V(\xi, \eta, \Phi) \cdot S_{mn}(\eta) \cdot \exp(im\Phi)\, d\Omega, \quad [10]$$

where Ω is the domain of η and Φ. Therefore we let

$$V = \frac{(-c)^m m!}{2\sqrt{2\pi}(2m)!} K_m(\kappa r)\cdot P_m^m(\cos\theta)\cdot\exp(-im\phi), \quad (n-m) \text{ is even}, \quad [11a]$$

$$V = \frac{(-1)^m c^{m+1} m!}{4\sqrt{2\pi}(2m+1)!} K_{m+1}(\kappa r)\cdot P_{m+1}^m(\cos\theta) \cdot\exp(-im\phi), \quad (n-m) \text{ is odd}, \quad [11b]$$

where $\{r, \theta, \phi\}$ represents the conventional spherical coordinate. Transforming these results into a spheroidal coordinate and substituting the resultant expressions into Eq. [10], we obtain

$$R_{m(m+2s)}(\xi) = (\xi^2 - j)^{m/2} \sum_{q=0}^{\infty} \omega_{2q} K_{m+q} \times \left[\frac{c}{2}(\xi + \sqrt{\xi^2 - j})\right]\cdot I_{m+q}\left[\frac{jc}{2}(\xi - \sqrt{\xi^2 - j})\right], \quad [12a]$$

$$R_{(m+2s+1)m}(\xi) = \xi(\xi^2 - j)^{m/2} \sum_{q=0}^{\infty} \omega_{2q+1} K_{m+q+1} \times \left[\frac{c}{2}(\xi + \sqrt{\xi^2 - j})\right]\cdot I_{m+q+1}\left[\frac{jc}{2}(\xi - \sqrt{\xi^2 - j})\right], \quad [12b]$$

where I is the modified spherical Bessel function of the first kind and

$$\omega_{2q} = (2m + 2q + 1)\sum_{s=0}^{q}\sum_{t=s}^{q}(-1)^{t+((1-j)q/2)} \frac{2^{m+2s+1}(2m+q+t)!(2m+2s)!(2t)!(t+m+s)!}{t!(m+t)!(q-t)!(2s)!(t-s)!(2t+2m+2s+1)!} A_{mn,2s} \quad [12c]$$

$$\omega_{2q+1} = (2m + 2q + 3)\sum_{s=0}^{q}\sum_{t=s}^{q}(-1)^{t+((1-j)q/2)} \cdot\frac{2^{m+2s+2}(2m+q+t+2)!(2m+2s+1)!(2t+1)!(t+m+s+1)!}{t!(m+t+1)!(q-t)!(2s+1)!(t-s)!(2t+2m+2s+3)!} A_{mn,2s+1}. \quad [12d]$$

C. Surface Conditions

We assume that the boundary conditions associated with Eq. [1] are the electrical potential vanishes as the distance from the charged surface approaches infinity and the charged condition at the surface needs to be satisfied. Due to the nature of the radial functions obtained, the former is satisfied automatically. For the latter, we consider a general expression of the form

$$h_1(\eta, \Phi)\cdot y + h_2(\eta, \Phi)\frac{\partial y}{\partial \xi} = f(\eta, \Phi), \quad \xi = \xi_s^+, \quad [13]$$

where

$$h_1 = \begin{cases} 1, & (\eta, \Phi) \in \Omega_p \\ 0, & (\eta, \Phi) \in \Omega_c \end{cases} \quad [13a]$$

$$h_2 = 1 - h_1. \quad [13b]$$

In these expressions, Ω_p and Ω_c denote, respectively, the region of constant potential and constant charge density on the surface of the particle. It can be shown that the angle functions S_{mn}, $m, n = 0, 1, \ldots$, defined in Eq. [4] are orthogonal functions (18). Although this nature can reduce significantly the difficulty of solving a nonuniform constant potential or constant surface charge problem (Appendix B), it can not be employed directly in the resolution of the present mixed boundary problem. Substituting Eq. [13] into Eq. [3] yields

$$f(\eta, \Phi) = \sum_{m=0}^{\infty}\sum_{n=m}^{\infty}[h_1 R_{mn}(\xi_s) + h_2 R'_{mn}(\xi_s)] \times S_{mn}(\eta)[C_{mn}\cos m\Phi + D_{mn}\sin m\Phi]. \quad [14]$$

If the rate of convergence of the right-hand side of this expression is sufficiently fast, only finite terms need to be considered. In this case, the coefficients C_{mn} and D_{mn} can be estimated by (19)

$$\int_\Omega \begin{bmatrix} \underline{f}^c \\ \underline{f}^s \end{bmatrix} d\Omega = \int_\Omega \begin{bmatrix} \underline{W}^c \\ \underline{W}^s \end{bmatrix} [\underline{M}^c \underline{M}^s] d\Omega \begin{bmatrix} \underline{C} \\ \underline{D} \end{bmatrix}, \quad [15]$$

where a symbol with an underbar denotes a vector. The elements of the vectors in this expression are defined by

$$f_i^c = f(\eta, \Phi)S_{mn}(\eta)\cos(m\Phi) \quad [15a]$$

$$f_i^s = f(\eta, \Phi)S_{mn}(\eta)\sin(m\Phi) \quad [15b]$$

$$W_i^c = S_{mn}(\eta)\cos(m\Phi) \quad [15c]$$

$$W_i^s = S_{mn}(\eta)\sin(m\Phi) \quad [15d]$$

$$M_j^c = [h_1 R_{mn}(\xi_s) + h_2 R'_{mn}(\xi_s)] S_{mn}(\eta)\cos(m\Phi) \quad [15e]$$

$$M_j^s = [h_1 R_{mn}(\xi_s) + h_2 R'_{mn}(\xi_s)] S_{mn}(\eta)\sin(m\Phi) \quad [15f]$$

$$C_i^c = C_{mn} \quad [15g]$$

$$D_i^c = D_{mn}. \quad [15h]$$

In these expressions, $mn = 00, 01, \ldots, 11, 12, \ldots, 22, 23, \ldots$, for $i = 1, 2, \ldots$. On the other hand, if the rate of convergence of the right-hand side of Eq. [14] is slow, the computation based on Eq. [15] becomes inefficient and another approach should be employed. Here, we suggest using the method of reflections (20), which is often adopted for the evaluation the interactions between two surfaces. In general, since two coordinate systems need to be considered simultaneously, the computational effort is appreciable. For the present case, however, the numerical work is limited because only one surface is considered.

The reflection method is of iterative nature. In the first stage we consider the boundary condition

$$y = h_1 f(\eta, \Phi). \quad [16]$$

The solution to Eq. [2] subject to this expression, $y^{(0)}$, is Eq. [B2] with

$$\begin{pmatrix} C_{mn}^{(0)} \\ D_{mn}^{(0)} \end{pmatrix} = \int_\Omega h_1 f(\eta, \Phi) S_{mn}(\eta) \begin{pmatrix} \cos m\Phi \\ \sin m\Phi \end{pmatrix} d\Omega. \quad [17]$$

The contribution to the surface charge density in region Ω_c due to $y^{(0)}$ is denoted by $\sigma_p^{(0)}$, which can be calculated by Eq. [B3]. Apparently, $\sigma_p^{(0)}$ needs to be subtracted from the exact surface charge density. In the second stage, Eq. [2] is solved subject to

$$y = h_2 f(\eta, \Phi). \quad [18]$$

The result, denoted by $y^{(1)}$, is Eq. [B5] with

$$\begin{pmatrix} C_{mn}^{(1)} \\ D_{mn}^{(1)} \end{pmatrix} = \int_\Omega h_2 [f(\eta, \Phi) + \sigma_p^{(0)} h_s'] S_{mn}(\eta) \begin{pmatrix} \cos m\Phi \\ \sin m\Phi \end{pmatrix} d\Omega. \quad [19]$$

The contribution to the surface potential in region Ω_p due to $y^{(1)}$ is expressed as $y_c^{(1)}$, which can be evaluated by Eq. [B6]. In the next stage, $y_c^{(1)}$ needs to be corrected from the exact potential distribution. The procedure is continued until a satisfactory result is obtained. In summary, we have

$$\begin{aligned} y &= y^{(0)} + y^{(1)} + y^{(2)} + \cdots \\ &= \sum_{m=0}^{\infty} \sum_{n=m}^{\infty} \frac{R_{mn}(\xi) S_{mn}(\eta)}{E_{mn} R_{mn}(\xi_s)} [(C_{mn}^{(0)} + C_{mn}^{(2)} \\ &\quad + \cdots)\cos m\Phi + (D_{mn}^{(0)} + D_{mn}^{(2)} + \cdots)\sin m\Phi] \\ &\quad + \sum_{m=0}^{\infty} \sum_{n=m}^{\infty} \frac{R_{mn}(\xi) S_{mn}(\eta)}{E_{mn} R'_{mn}(\xi_s)} [(C_{mn}^{(1)} + C_{mn}^{(3)} \\ &\quad + \cdots)\cos m\Phi + (D_{mn}^{(1)} + D_{mn}^{(3)} + \cdots)\sin m\Phi] \end{aligned} \quad [20]$$

with

$$\begin{pmatrix} C_{mn}^{(i+1)} \\ D_{mn}^{(i+1)} \end{pmatrix} = -\int_\Omega h_1 y_c^{(i)} S_{mn}(\eta) \begin{pmatrix} \cos m\Phi \\ \sin m\Phi \end{pmatrix} d\Omega, \quad i = 1, 3, \ldots \quad [20a]$$

$$\begin{pmatrix} C_{mn}^{(i+1)} \\ D_{mn}^{(i+1)} \end{pmatrix} = -\int_\Omega h_2 [\sigma_p^{(i)} h_s'] S_{mn}(\eta) \begin{pmatrix} \cos m\Phi \\ \sin m\Phi \end{pmatrix} d\Omega, \quad i = 2, 4, \ldots. \quad [20b]$$

3. DISCUSSION

Colloidal particles can assume various shapes. The infinite plate, long cylinder, and sphere often assumed in the conventional analyses are idealized models. The spheroidal geometry adopted in the present study is capable of providing a more general description for the problem under consideration. As illustrated in Fig. 1, by varying the value of ξ, various types of surfaces can be simulated, ranging from needle-like or disk-like to spherical surfaces.

The constant $c(=\kappa a)$ is one of the major parameters in the present analysis. As suggested by Flammer (5), its value should not exceed 10. Evaluating R_{mn} and S_{mn} in Eq. [3] becomes nontrivial if c is large. However, a large value of c implies that the electrical double layer is thin. In this case, a double layer can be considered planar, the result of which is well known. In other words, the present analysis is more appropriate for a relatively thick double layer.

Table 1 shows the typical variation of $A_{mn,s}$. The results presented in this table reveal that the rate of convergence of the right-hand side of Eq. [4] is fast. This suggests that employing Eqs. [5a]–[5c] is more efficient than using the approach reported in the literatures (5, 6). The latter involves solving transcendental equations numerically, which can be time consuming.

A surface having nonuniform surface charged properties is not uncommon for mineral and biological colloids. Figure 2 shows an example for a surface with patchwise charge distribution. This distribution is assumed as

TABLE 1
Values of $A_{mn,s}$ in Eq. [4] for the Case $c^2 = 2$

$A_{mn,s}$											
m	n	s:	0, 1	2, 3	4, 5	6, 7	8, 9	10, 11	12, 13	14, 15	16, 17
0	0		1.000E + 00	2.352E − 01	8.183E − 03	1.189E − 04	9.519E − 07	4.835E − 09	1.697E − 11	4.363E − 14	8.574E − 17
	1		1.000E + 00	7.847E − 02	1.766E − 03	1.913E − 05	1.225E − 07	5.185E − 10	1.561E − 12	3.515E − 15	6.144E − 18
	2		−4.709E − 02	1.000E + 00	4.904E − 02	8.257E − 04	7.186E − 06	3.850E − 08	1.403E − 10	3.709E − 13	7.445E − 16
	3		−3.364E − 02	1.000E + 00	3.528E − 02	4.710E − 04	3.410E − 06	1.567E − 08	5.000E − 11	1.176E − 13	2.128E − 16
	4		3.685E − 04	−2.717E − 02	1.000E + 00	2.755E − 02	3.044E − 04	1.884E − 06	7.574E − 09	2.150E − 11	4.554E − 14
1	1		1.000E + 00	2.814E − 02	3.906E − 04	3.067E − 06	1.541E − 08	5.372E − 11	1.375E − 13	2.691E − 16	4.162E − 19
	2		1.000E + 00	2.466E − 02	2.776E − 04	1.815E − 06	7.790E − 09	2.367E − 11	5.367E − 14	9.432E − 17	1.323E − 19
	3		−7.239E − 02	1.000E + 00	2.123E − 02	2.027E − 04	1.142E − 06	4.297E − 09	1.161E − 11	2.368E − 14	3.780E − 17
	4		−4.567E − 02	1.000E + 00	1.839E − 02	1.525E − 04	7.555E − 07	2.531E − 09	6.159E − 12	1.142E − 14	1.671E − 17
2	2		1.000E + 00	8.476E − 03	5.808E − 05	2.735E − 07	9.177E − 10	2.290E − 12	4.406E − 15	6.725E − 18	8.335E − 21
	3		1.000E + 00	1.070E − 02	6.843E − 05	2.901E − 07	8.746E − 10	1.972E − 12	3.451E − 15	4.824E − 18	5.511E − 21
	4		−7.065E − 02	1.000E + 00	1.107E − 02	6.571E − 05	2.536E − 07	6.958E − 10	1.434E − 12	2.305E − 15	2.977E − 18
3	3		1.000E + 00	3.624E − 03	1.402E − 05	4.266E − 08	1.004E − 10	1.856E − 13	2.754E − 16	3.342E − 19	3.373E − 22
	4		1.000E + 00	5.570E − 03	2.211E − 05	6.416E − 08	1.411E − 10	2.425E − 13	3.345E − 16	3.783E − 19	3.569E − 22
	5		−6.457E − 02	1.000E + 00	6.491E − 03	2.554E − 05	7.044E − 08	1.453E − 10	2.336E − 13	3.015E − 16	3.195E − 19
4	4		1.000E + 00	1.874E − 03	4.486E − 06	9.329E − 09	1.599E − 11	2.253E − 14	2.634E − 17	2.584E − 20	2.153E − 23
	5		1.000E + 00	3.259E − 03	8.572E − 06	1.777E − 08	2.936E − 11	3.937E − 14	4.358E − 17	4.044E − 20	3.188E − 23
	6		−5.838E − 02	1.000E + 00	4.125E − 03	1.131E − 05	2.306E − 08	3.666E − 11	4.688E − 14	4.930E − 17	4.342E − 20

FIG. 2. An example showing the patchwise distribution of the dimensionless surface charges for the case $\xi_s = 1.02$, $c^2 = 2$, $a = 1$, and $u = 1$.

$$\sigma = u/h_s'\{\exp[\sin(1.5\Phi)\sin(2\pi\eta)] - 1\} + \sigma_{00}\cdot(1 - u), \quad 0 \leqslant u \leqslant 1, \quad [21]$$

where σ_{00} denotes the mean surface charge. It can be shown that this expression leads to a fixed total amount of charges, which is independent of u. Here, u is a measure of the degree of nonuniformity of the distribution of charges. The smaller its value, the more uniform the distribution of charges. If $u = 0$, the surface charges are distributed uniformly. Figure 2 shows the patchwise charge distribution for the case $u = 1$, and the corresponding distribution of surface potential is shown in Fig. 3.

If an uncharged surface is chosen as the reference state, the dimensionless Helmholtz free energy of the electrical double layer around a charged surface, F_{el}, can be calculated by

FIG. 3. Distribution of dimensionless surface potential for the case of Fig. 2.

$$F_{el} = \frac{1}{2}\int_{\Omega} y_s \sigma d\Omega, \qquad [22]$$

where

$$F_{el} = 16\pi e^2 f_{el}/(a\epsilon k_B^2 T^2), \qquad [22a]$$

f_{el} being the Helmholtz free energy of the double layer. Figure 4 shows the effect of the degree of nonuniformity of surface charge distribution on the dimensionless Helmholtz free energy of the electrical double layer. It reveals that neglecting the distribution of surface charges may lead to a significant deviation. In other words, using the averaged surface property to describe its behavior is unsatisfactory (21).

In general, obtaining an explicit form for the potential distribution from Eq. [21] can be nontrivial. Under certain circumstances, however, this can be achieved. Three examples are considered to illustrate the present approach. The first example is shown in Fig. 5a. The left semisurface of a spheroid remains at constant potential, and the rest of the spheroidal surface at constant charge density. In this case, the surface condition Eq. [13a] becomes

$$h_1 = \begin{cases} 1, & -1 \leqslant \eta \leqslant 1,\ 0 \leqslant \Phi \leqslant \pi \\ 0, & -1 \leqslant \eta \leqslant 1,\ \pi \leqslant \Phi \leqslant 2\pi. \end{cases} \qquad [23]$$

It can be shown that the solution to Eq. [2] subject to Eqs. [23] and [13b] is

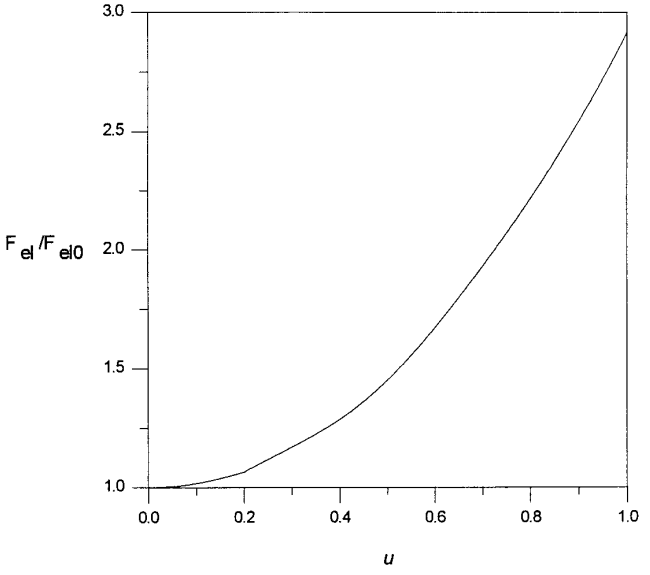

FIG. 4. Effect of the degree of uniformity of the surface condition measured by parameter u on the dimensionless Helmholtz free energy of double layer, F_{el}. The greater the value of u, the more nonuniform the distribution of surface charges. F_{el0} is the value of F_{el} when $u = 0$.

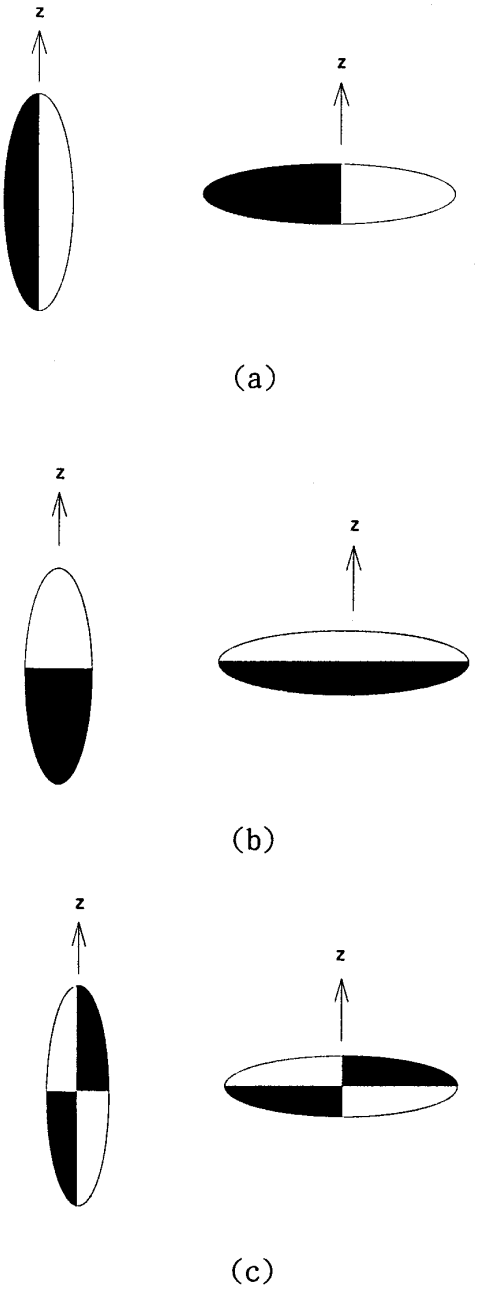

FIG. 5. Boundary conditions specified in the numerical simulations. Shaded regions are maintained at constant potential and the rest at constant charge: (a) example 1; (b) example 2; (c) example 3.

$$y = \sum_{m=0}^{\infty}\sum_{n=m}^{\infty} \frac{h_1 R_{mn}(\xi_s) + h_2 R'_{mn}(\xi_s)}{R_{mn}(\xi_s) + R'_{mn}(\xi_s)} \frac{S_{mn}(\eta)}{E_{mn}} \times (C_{mn}\cos m\Phi + D_{mn}\sin m\Phi), \qquad [24]$$

with

$$\begin{pmatrix} C_{mn} \\ D_{mn} \end{pmatrix} = \int_{\Omega} f(\eta, \Phi) S_{mn}(\eta) \begin{pmatrix} \cos m\Phi \\ \sin m\Phi \end{pmatrix} d\Omega \qquad [24a]$$

$$E_{mn} = w\pi \sum_{s=0,1}^{\infty} A_{mn,s}^2 \frac{(2m+s)!}{(2m+2s+1)s!}, \quad [24b]$$

where w is 2 if $m = 0$ and 1 if $m \neq 0$.

In the second example, the lower semisurface of a spheroid remains at constant potential, and the rest of the spheroidal surface at constant charge density, as illustrated in Fig. 5b. Here, Eq. [13a] reduces to

$$h_1 = \begin{cases} 1, & -1 \leqslant \eta \leqslant 0,\ 0 \leqslant \Phi \leqslant 2\pi \\ 0, & 0 \leqslant \eta \leqslant 1,\ 0 \leqslant \Phi \leqslant 2\pi. \end{cases} \quad [25]$$

If $f(\eta, \Phi)$ is either an even or an odd function with respect to η, the solution of Eq. [2] subject to Eqs. [25] and [13b] becomes

$$y = \sum_{m=0}^{\infty} \sum_{n=m,m+1}^{\infty} \frac{h_1 R_{mn}(\xi_s) + h_2 R'_{mn}(\xi_s)}{R_{mn}(\xi_s) + R'_{mn}(\xi_s)} \frac{S_{mn}(\eta)}{E_{mn}} \times (C_{mn}\cos m\Phi + D_{mn}\sin m\Phi), \quad [26]$$

where C_{mn}, D_{mn}, and E_{mn} are defined in Eqs. [24a] and [24b]; $(n - m)$ is even when $f(\eta, \Phi)$ is even with respect to η and is odd if $f(\eta, \Phi)$ is odd with respect to η.

The third example is illustrated in Fig. 5c. Two of the quadrant surfaces remain at constant potential, and the rest of the surface at constant charge. In this case, the associated boundary condition is

$$h_1 = \begin{cases} 1, & -1 \leqslant \eta \leqslant 0,\ 0 \leqslant \Phi \leqslant \pi \text{ and} \\ & \quad 0 \leqslant \eta \leqslant 1,\ \pi \leqslant \Phi \leqslant 2\pi \\ 0, & 0 \leqslant \eta \leqslant 1,\ 0 \leqslant \Phi \leqslant \pi \text{ and} \\ & \quad -1 \leqslant \eta \leqslant 0,\ \pi \leqslant \Phi \leqslant 2\pi. \end{cases} \quad [27]$$

It can be shown that if $f(\eta, \Phi)$ is either an even or an odd function with respect to η, the solution of Eq. [2] subject to Eqs. [27] and [13b] is Eq. [26].

The efficiency of the present reflection method can be improved by considering the following perturbation functions:

$$h_1 = \begin{cases} 1, & (\eta, \Phi) \in \Omega_p \\ \epsilon_1, & (\eta, \Phi) \in \Omega_c \end{cases} \quad [28a]$$

$$h_2 = \begin{cases} \epsilon_2, & (\eta, \Phi) \in \Omega_p \\ 1, & (\eta, \Phi) \in \Omega_c. \end{cases} \quad [28b]$$

Here ϵ_1 and ϵ_2 are two adjustable parameters. For example, suppose that the potential specified over the region Ω_p is positive. Then the reflection method will yield some positive deviation in the surface charge over the region Ω_c. In this case, assigning a small negative value to ϵ_1 has the effect of correcting this deviation, and the rate of convergence can be accelerated.

Evaluating the electrical potential distribution around a charged surface is the first step to various applications. In electrophoresis, for example, if the deformation of the electrical double layer near a charged particle caused by the relative motion between the particle and the surrounding fluid is neglected (Reynolds number $\ll 1$), its mobility can be estimated in a direct manner once the electrical potential distribution is known (7). The stability of a dispersed system is closely related to the electrical interaction between two dispersed entities. For a lean dispersion, the electrical potential distribution around a single charged entity provides sufficient information for this interaction. The result obtained in the present study is for a general application and is not limited to a specific problem.

APPENDIX A

If c^2 is sufficiently small, S_{mn} and λ_{mn} can be expanded as

$$S_{mn} = \sum_{r=0}^{\infty} S_{mn,r}(jc^2)^r \quad [A1a]$$

$$\lambda_{mn} = \sum_{r=0}^{\infty} \lambda_{mn,r}(jc^2)^r. \quad [A1b]$$

Note that if c^2 vanishes, Eq. [3a] reduces to the associated Legendre equation. This implies that $S_{mn,0} = P_n^m$ and $\lambda_{mn,0} = n(n+1)$. Substituting Eqs. [A1a] and [A1b] into Eq. [3a] yields the recursive equation

$$\frac{d}{d\eta}\left[(1-\eta^2)\frac{dS_{mn,r}}{d\eta}\right] + \eta^2 S_{mn,r-1} + \sum_{p=0}^{r} \lambda_{mn,p} S_{mn,r-p} = 0, \quad r \geqslant 1. \quad [A2]$$

Expanding $S_{mn,r}$ in associated Legendre functions, we have

$$S_{mn,r} = \sum_{s=0,1}^{\infty} a_{mn,r,s} P_{m+s}^m, \quad [A3]$$

where s is even if $(n - m)$ is even, and odd if $(n - m)$ is odd. It can be shown that

$$xP_n^m(x) = \frac{n-m+1}{2n+1} P_{n+1}^m(x) + \frac{n+m}{2n+1} P_{n-1}^m(x). \quad [A4]$$

Substituting Eq. [A3] into Eq. [A2], employing Eq. [A4], and combining the resultant expression with Eq. [A1], Eq. [4] can be recovered.

APPENDIX B

For a surface of constant potential

$$y = y_s(\eta, \Phi), \ \xi = \xi_s. \qquad [B1]$$

Solving Eq. [2] subject to this expression yields

$$y = \sum_{m=0}^{\infty} \sum_{n=m}^{\infty} \frac{R_{mn}(\xi) S_{mn}(\eta)}{E_{mn} R_{mn}(\xi_s)} \times (C_{mn} \cos m\Phi + D_{mn} \sin m\Phi) \qquad [B2]$$

with

$$\begin{pmatrix} C_{mn} \\ D_{mn} \end{pmatrix} = \int_{\Omega} y_s(\eta, \Phi) S_{mn}(\eta) \begin{pmatrix} \cos m\Phi \\ \sin m\Phi \end{pmatrix} d\Omega \qquad [B2a]$$

$$E_{mn} = w\pi \sum_{s=0,1}^{\infty} A_{mn,s}^2 \frac{(2m + s)!}{(2m + 2s + 1)s!}, \qquad [B2b]$$

where w is 4 if $m = 0$ and 2 if $m \neq 0$. The corresponding dimensionless surface charge is

$$\sigma = \sum_{m=0}^{\infty} \sum_{n=m}^{\infty} \frac{R'_{mn}(\xi) S_{mn}(\eta)}{h'_s E_{mn} R_{mn}(\xi_s)} \times (C_{mn} \cos m\Phi + D_{mn} \sin m\Phi), \qquad [B3]$$

where

$$\sigma = \frac{4\pi e a \sigma'}{\epsilon k_B T} \qquad [B3a]$$

$$h'_s = \sqrt{\frac{\xi_s^2 - j\eta^2}{\xi_s^2 - j}}. \qquad [B3b]$$

Suppose that a surface remains at constant charges. Let $\sigma'(\eta, \Phi)$ be the distribution of charges on the surface. Applying the Gauss law yields

$$\vec{n} \cdot \vec{\nabla} y = -\frac{4\pi e \sigma'(\eta, \Phi)}{\epsilon k_B T}, \text{ at } \xi = \xi^+, \qquad [B4]$$

where $\vec{n}$ and $\vec{\nabla}$ are, respectively, the unit outer normal of the surface and the gradient operator. The solution of Eq. [2] subject to Eq. [B4] is

$$y = \sum_{m=0}^{\infty} \sum_{n=m}^{\infty} \frac{R_{mn}(\xi) S_{mn}(\eta)}{E_{mn} R'_{mn}(\xi_s)} \times (C_{mn} \cos m\Phi + D_{mn} \sin m\Phi), \qquad [B5]$$

where E_{mn} is defined in Eq. [B2b] and

$$\begin{pmatrix} C_{mn} \\ D_{mn} \end{pmatrix} = -\int_{\Omega} \sigma(\eta, \Phi) h'_s S_{mn}(\eta) \begin{pmatrix} \cos m\Phi \\ \sin m\Phi \end{pmatrix} d\Omega. \qquad [B5a]$$

The corresponding dimensionless surface potential is

$$y_s = \sum_{m=0}^{\infty} \sum_{n=m}^{\infty} \frac{R_{mn}(\xi_s) S_{mn}(\eta)}{E_{mn} R'_{mn}(\xi_s)} \times (C_{mn} \cos m\Phi + D_{mn} \sin m\Phi). \qquad [B6]$$

ACKNOWLEDGMENT

This work is supported by the National Science Council of the Republic of China under project NSC84-2214-E002-005.

REFERENCES

1. Hunter, R. J., *in* ''Foundations of Colloid Science,'' Vol. 1. Oxford University, London, 1989.
2. Fair, M. C., and Anderson, J. L., *J. Colloid Interface Sci.* **127,** 388 (1989).
3. Feng, J. J., and Wu, W. Y., *J. Fluid Mech.* **264,** 41 (1994).
4. Keh, H. J., and Huang, T. Y., *J. Colloid Interface Sci.* **160,** 354 (1993).
5. Flammer, C., *in* ''Spheroidal Wave Functions.'' Stanford Univ. Press, Stanford, CA, 1957.
6. Stratton, J. A., Morse, P. M., Chu, L. J., Little, J. D. C., and Corbato, F. J., *in* ''Spheroidal Wave Functions.'' Wiley, New York, 1956.
7. Yoon, B. J., and Kim, S., *J. Colloid Interface Sci.* **128,** 275 (1989).
8. Hus, J. P., and Liu, B. T., *J. Colloid Interface Sci.* **175,** 785 (1996).
9. Grim, R. E., *in* ''Applied Clay Mineralogy.'' McGraw-Hill, New York, 1962.
10. Ninham, B. W., and Parsegian, V. A., *J. Theor. Biol.* **31,** 405 (1971).
11. Chan, D., Perram, J. W., White, L. R., and Healy, T. W., *J. Chem. Soc. Faraday Trans. I* **71,** 1046 (1975).
12. Chan, D., Perram, J. W., and White, L. R., *J. Chem. Soc. Faraday Trans. I* **72,** 2844 (1976).
13. Wang, T. K., and Audebert, R., *J. Colloid Interface Sci.* **119,** 459 (1987).
14. Moon, P., and Spencer, D. E., *in* ''Field Theory Handbook.'' Springer-Verlag, Berlin, 1961.
15. Watson, G. N., *in* ''Theory of Bessel Functions.'' Cambridge Univ. Press, Cambridge, UK, 1922.
16. Aoi, T., *J. Phys. Soc. Jpn.* **10,** 130 (1955).
17. Abramowitz, M., and Stegun, I. A., *in* ''Handbook of Mathematical Functions.'' Dover, New York, 1965.
18. Hildebrand, F. B., *in* ''Methods of Applied Mathematics,'' 2nd ed. Prentice Hall, Englewood Cliffs, NJ, 1965.
19. Hsu, J. P., and Tseng, M. T., *J. Chem. Phys.* **104,** 242 (1996).
20. Happel, J., and Brenner, H., *in* ''Low Reynolds Number Hydrodynamics.'' Prentice Hall, Englewood Cliffs, NJ, 1965.
21. Miklavic, S. J., Chan, D. Y. C., White, L. R., and Healy, T. W., *J. Phys. Chem.* **98,** 9022 (1994).